

Strange Mesons in Dense Nuclear Matter

Peter Senger ^a

^aGSI, Planckstr.1, 64291 Darmstadt

Experimental data on the production of kaons and antikaons in heavy ion collisions at relativistic energies are reviewed with respect to in-medium effects. The K^-/K^+ ratios measured in nucleus-nucleus collisions are 1 - 2 orders of magnitude larger than in proton-proton collisions. The azimuthal angle distributions of K^+ mesons indicate a repulsive kaon-nucleon potential. Microscopic transport calculations consistently explain both the yields and the emission patterns of kaons and antikaons when assuming that their properties are modified in dense nuclear matter. The K^+ production excitation functions measured in light and heavy collision systems provide evidence for a soft nuclear equation-of-state.

1. Strangeness in neutron stars and nuclear fireballs

Heavy-ion collisions at relativistic energies provide the unique possibility to create a dense and hot nuclear system which can be investigated experimentally. In a reaction between two gold nuclei at a beam energy of 1 AGeV, for example, a fireball is produced with baryonic densities up to 3 times saturation density and temperatures around 100 MeV. Although this transient state exists only for about 10-20 fm/c, it offers the opportunity to catch a glimpse of nuclear matter far off its ground state. In nature, similarly extreme conditions exist only in the interior of neutron stars. Therefore, experiments at heavy ion accelerators allow to address questions which could not be answered before. The nuclear equation-of-state at high baryon densities and the properties of hadrons in dense nuclear matter are essential for our understanding of astrophysical phenomena such as the dynamics of a supernova and the stability of neutron stars. Moreover, heavy-ion experiments may shed light on the question whether chiral symmetry is (partly) restored at high baryon densities. The study of hadron properties in dense nuclear matter will help to explore a fundamental problem of strong-interaction physics that is the mechanism which dynamically breaks chiral symmetry and generates hadron masses.

Strange mesons are regarded as promising probes both for the study of the in-medium properties of hadrons and the nuclear equation-of-state [1,2]. Figure 1 displays the range of predictions of various model calculations for the total energy of K mesons at rest in nuclear matter as function of density (see [3]). According to the calculations, the effective mass of a K^+ meson increases moderately with increasing baryon density whereas the effective mass of K^- mesons decreases significantly. In mean-field calculations, this effect is caused by a repulsive K^+N potential and an attractive K^-N potential. Microscopic

calculations predict a dynamical broadening of the K^- meson spectral function which is shifted towards smaller energies [4,5]. The ultimate goal is to relate the in-medium spectral function of kaons and antikaons to the anticipated chiral symmetry restoration at high baryon density (for details see the contribution of G. Chanfray).

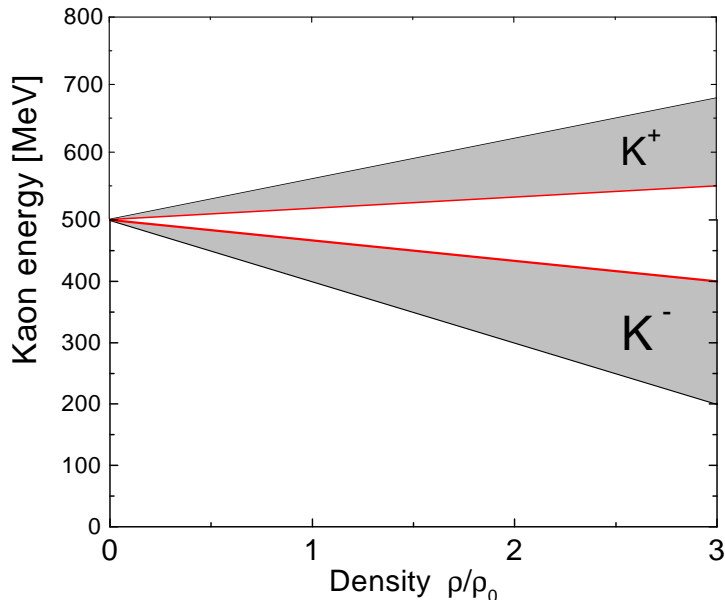


Figure 1. *Effective in-medium mass of kaons and antikaons as function of nuclear density. The grey shaded areas represent the range of predictions of various calculations (see [3]).*

H. Bethe and G. Brown pointed out that a strong decrease of the K^- effective mass with increasing baryon density should have dramatic consequences for the stability of neutron stars [6–8]. Above a certain value of baryon density (≈ 3 times saturation density ρ_0) the total energy of a K^- meson might become smaller than the electrochemical potential ($\mu_e \approx 230$ MeV). Then K^- mesons will replace the electrons and form a Bose condensate. The condensation of negative bosons enhances the proton to neutron ratio and this effect softens the equation-of-state. Consequently, a supernova core with 1.5 - 2 solar masses will collapse into a black hole rather than form a neutron star [6]. This mechanism would explain the observation that the masses of binary pulsars do not exceed significantly the value of 1.5 solar masses.

The predicted behavior of K mesons in dense matter as illustrated in figure 1 has not yet been confirmed experimentally. The analysis of data on K^+ -nucleus scattering [9] and kaonic atoms [10] found evidence for sizeable KN potentials at saturation density and below. Higher densities – which are of interest for astrophysics – can only be investigated by heavy-ion experiments.

The challenge is to find experimental observables which can be related quantitatively to the searched in-medium effects. If the total energy of K mesons is modified in dense nuclear matter according to figure 1, then the energy threshold for K meson production will be modified as well. K^+ and K^- can hardly be produced in direct nucleon-nucleon collisions at beam energies below the threshold which is 1.58 GeV for the reaction $NN \rightarrow K^+\Lambda N$ and 2.5 GeV for $NN \rightarrow K^+K^-NN$. Therefore, kaon production excitation function rises steeply with increasing beam energy close to and below threshold. This steep rise amplifies the effect of a modified in-medium mass on the K meson yield. A moderate enhancement of the K^+ effective mass of about 10% will result in an enhanced threshold and, hence, in a reduction of the K^+ yield by about a factor of 2. In contrast, the K^- yield will be strongly enhanced as the effective mass is expected to be reduced substantially (see figure 1). In addition, the absorption probability of K^- mesons via the strangeness exchange reaction $K^-N \rightarrow Y\pi$ (with $Y = \Lambda, \Sigma$) will be reduced if the K^- effective mass decreases. Therefore, the yield of kaons and antikaons produced in heavy-ion collisions at beam energies below threshold is sensitive to their effective in-medium masses. Measured cross sections can be quantitatively compared to the results of transport calculations which take into account also the properties of the fireball matter such as density, compressibility and abundance of excited nucleons.

Another measurable effect of in-medium KN potentials is their influence on the propagation of kaons and antikaons in heavy-ion collisions. K^+ mesons – which cannot be absorbed as they contain an antistrange quark – will be repelled from the regions of increased baryonic density because of the repulsive K^+N potential. In contrast, K^- mesons will be attracted [11]. Therefore, the azimuthal emission pattern of K mesons is expected to be modified according to the in-medium KN potentials and the density profile of the nuclear medium.

Experiments on kaon and antikaon production and propagation in heavy-ion collisions at relativistic energies have been performed with the Kaon Spectrometer [12] and the FOPI detector [13] at the heavy-ion synchrotron SIS at GSI Darmstadt. Results have been published in [14–21]. The most recent results will be presented in this contribution. The paper is organized as follows: In section 2 we show that kaons are created predominantly at high baryon densities. In section 3 we present evidence for in-medium effects on the K meson yields and compare data to results of microscopic transport calculations. In section 4 we discuss the influence of in-medium potentials on the azimuthal emission pattern of K mesons. In section 5 we show experimental results on K^+ production which indicate that the nuclear equation-of-state is soft. Finally, we present a conclusion and an outlook.

2. Kaons as messengers from the dense nuclear fireball

In order to obtain information on the high-density phase of a nucleus-nucleus collision one should measure particles which are created predominantly in this phase. This condition is fulfilled for K^+ mesons as illustrated in figure 2 which shows the results of a RBUU calculation for a central Au+Au collision at a beam energy of 1 AGeV [22]. The baryon density in the fireball reaches a value of almost three times saturation density ρ_0 . The lower part of figure 2 demonstrates that K^+ mesons are produced while the baryon density exceeds a value of twice ρ_0 . This is due to K^+ production via secondary collisions such as $\pi N \rightarrow K^+ \Lambda$ or $\Delta N \rightarrow K^+ \Lambda N$ which happen mostly at high baryon densities.

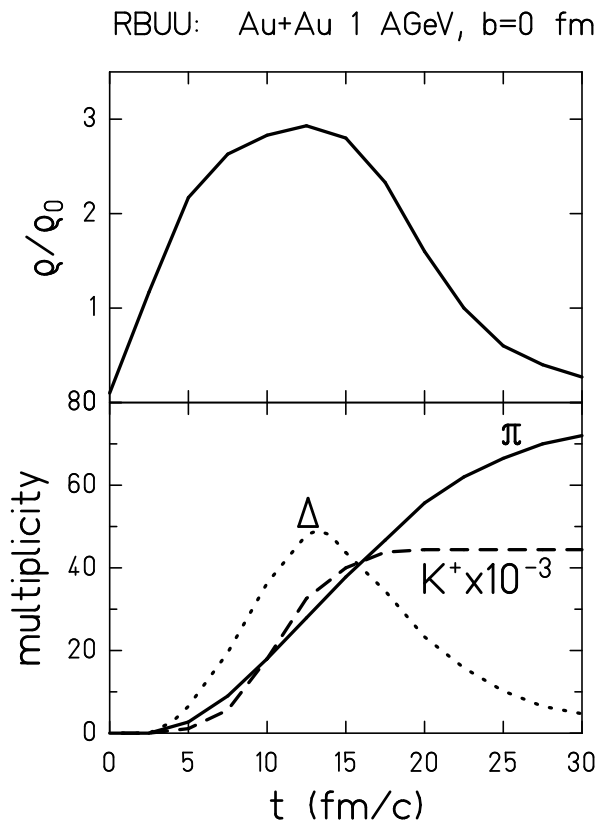


Figure 2. *Upper panel: time evolution of the baryon density (nucleons and Δ -resonances) in the fireball of a central Au+Au collision at a beam energy of 1 A·GeV.*

Below: multiplicity of Δ -resonances (dotted line), pions (solid line) and K^+ mesons (dashed line) as function of time (RBUU-calculation, taken from [22]).

Figure 2 cannot be proved directly by experiment as the baryon density is not an observable. However, the density dependence of K^+ production can be studied indirectly by measuring the K^+ yield as function of the collision centrality. Figure 3 shows the π^+ and K^+ multiplicities per number of participating nucleons A_{part} as function of A_{part} measured in Au+Au collisions at 1 AGeV by the KaoS Collaboration [23]. In contrast to the pions, the K^+ multiplicity clearly increases more than linearly with A_{part} . This finding indicates that the nucleons participate more than once in K^+ production. Such multiple collisions are strongly enhanced at high densities.

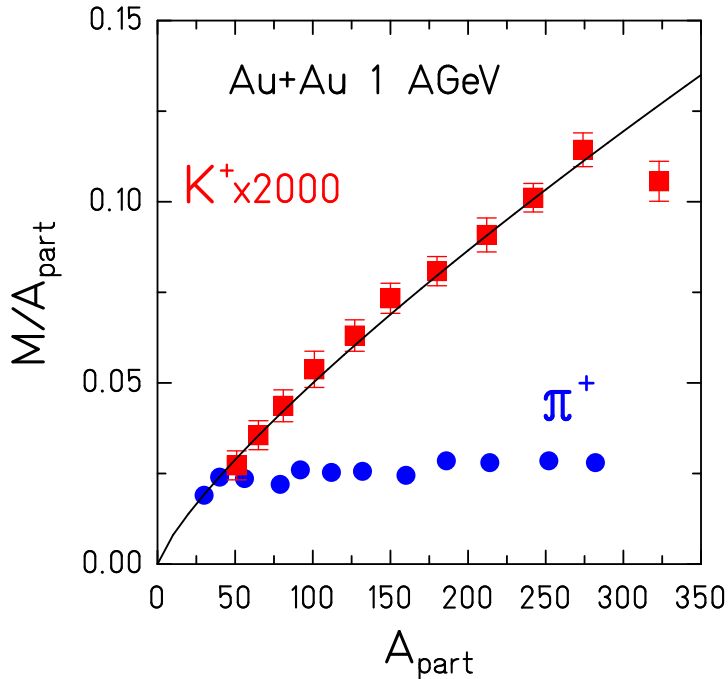


Figure 3. K^+ and π^+ multiplicity per participating nucleon M/A_{part} as a function of A_{part} for Au+Au collisions at 1 AGeV [23]. The data are taken at $\Theta_{lab}=44^\circ$ and extrapolated to the full solid angle assuming an isotropic angular distribution in the center-of-mass system. The line corresponds to a parameterization according to $M_{K^+} \propto A_{part}^{1.8}$.

3. In-medium effects on kaon and antikaon yields

In this section we review experimental data on K^+ and K^- yields as function of beam energy and the size of the collision system. We confront measured K^+ and K^- phase-space distributions with results of transport model calculations.

In order to see indications for in-medium effects on K^+ and K^- production we compare nucleus-nucleus to proton-proton collisions. Fig. 4 shows the multiplicity of K^+ and K^- mesons per average number of participating nucleons $M_K / \langle A_{part} \rangle$ as function of the Q-value in the NN system. The data were measured in C+C and Ni+Ni collisions by the KaoS Collaboration [17,20,24]. The Q-value is defined as the energy above threshold. The lines represent parameterizations of the available proton-proton data averaged over the isospin channels [25–27]. In "nucleon-nucleon" collisions the kaon multiplicity exceeds the antikaon multiplicity by 1-2 orders of magnitudes at the same Q-value. This large difference has disappeared for nucleus-nucleus collisions where the kaon and antikaon data nearly fall on the same curve. This observation indicates that the production of antikaons is strongly enhanced in nucleus-nucleus collisions.

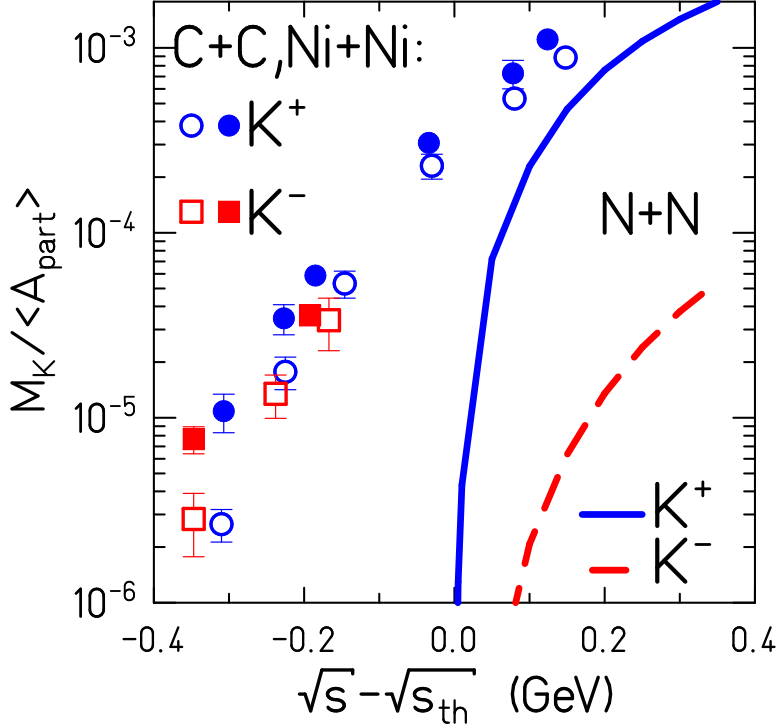


Figure 4. K^+ (circles) and antikaon (squares) multiplicity per participating nucleon as a function of the Q-value for C+C (open symbols) and Ni+Ni (full symbols) collisions [17,20,24]. The lines correspond to parameterizations of the production cross sections for K^+ (solid) and K^- (dashed) in nucleon-nucleon collisions [25–27].

In the following we discuss the possibility to study in-medium effects in K meson production by varying the size of the collision system. Figure 5 presents the K^-/K^+ ratio measured in C+C, Ni+Ni and Au+Au collisions at a beam energy of 1.5 AGeV [20,24,28]. The ratio is approximately constant for the three systems, although the reabsorption probability for K^- mesons should be very different: The K^- mean free path is about 1.5 fm at saturation density. In a geometrical model, the losses of K^- mesons due to strangeness exchange $K^-N \rightarrow Y\pi$ are estimated to be more than 10 times larger in Au than in C nuclei. Therefore, the data in figure 5 suggest that in the Au+Au system the absorption of K^- is compensated by an enhanced production and/or that the K^- absorption process is suppressed. Both effects can be caused by a reduced in-medium effective mass of antikaons.

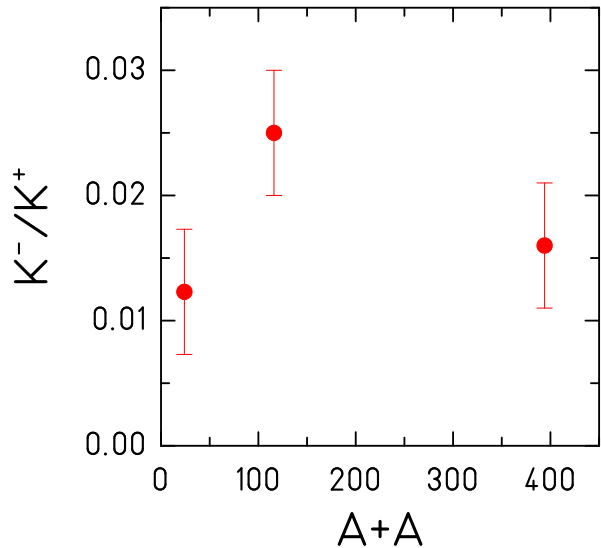


Figure 5. K^-/K^+ ratio measured in C+C, Ni+Ni and Au+Au collisions at a beam energy of 1.5 AGeV (preliminary) [20,24,28].

Now we compare measured phase-space distributions of K^- and K^+ mesons to the results of transport codes in order to analyze more quantitatively the in-medium effects. Figure 6 shows the K^+ and K^- multiplicity densities dN/dy and their ratio for near-central Ni+Ni collisions at 1.93 AGeV as function of the rapidity y_{CM} . The rapidity is defined here as $y_{CM} = y - 0.5 \times y_{proj}$. The value $y_{CM} = 0$ corresponds to midrapidity and $y_{CM} = \pm 0.89$ to projectile or target rapidity, respectively. Figure 6 combines data measured by the KaoS Collaboration (circles) [24] and by the FOPI Collaboration (squares) [18,29]. The KaoS data were analyzed for the most central 620 ± 30 mb of the reaction cross section (corresponding to impact parameters smaller than $b = 4.4$ fm in a sharp cutoff model) whereas the FOPI data were analysed for the most central 350 mb ($b = 3.3$ fm). Therefore, the FOPI multiplicities should be higher by about 20%. Nevertheless, the K^+ multiplicity densities and the K^-/K^+ ratios measured by the two experiments in the overlapping rapidity range agree with each other within the experimental errors.

The data are compared to results of RBUU transport calculations performed by Li and Brown (grey lines [30]) and Cassing and Bratkovskaya (black lines [31]). The dashed lines represent the results of calculations with bare kaon and antikaon masses whereas the solid lines are calculated with in-medium masses. The "bare mass" calculations clearly overestimate the K^+ yield and underestimate the K^- yield. The results of the "in-medium" calculations reproduce well the K^+ data but not the K^- data which are overestimated by Li and Brown and underestimated by Cassing and Bratkovskaya. The data now allow for a fine tuning of the strength of the K^-N potential which is a free parameter in those models.

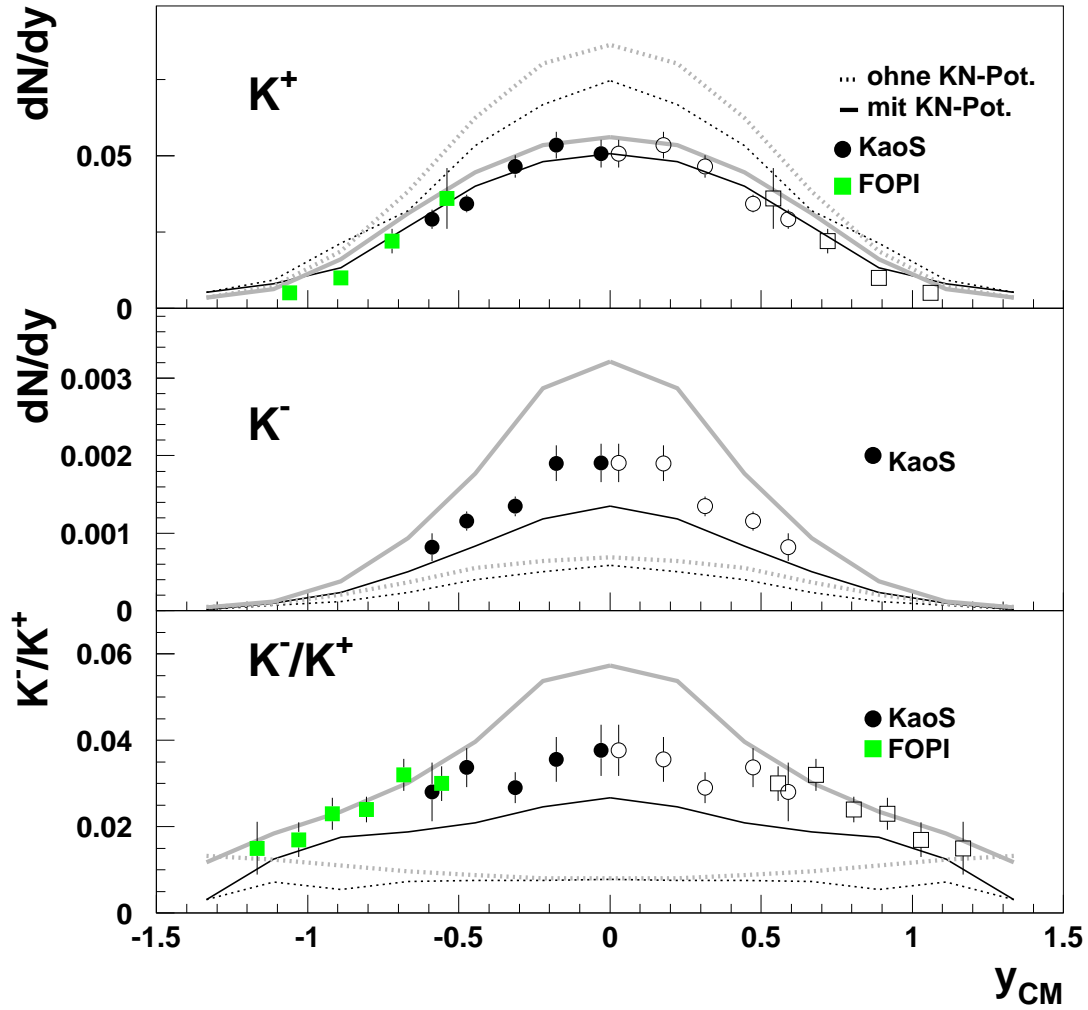


Figure 6. Multiplicity density distributions of K^+ (upper panel) and K^- mesons (center panel) for near-central ($b < 4.4$ fm) Ni+Ni collisions at 1.93 AGeV. Circles: KaoS data [24], squares: FOPI data [18,29]. The measured data (full symbols) are mirrored at $y_{CM}=0$ (open symbols). Lower panel: K^-/K^+ ratio. The data are compared to BUU transport calculations (black lines [31], grey lines [30]). Solid lines: with in-medium effects. Dotted lines: without in-medium effects.

4. In-medium effects on the emission pattern of K^+ mesons

In this section we discuss the influence of the in-medium KN potentials on the propagation of K^+ mesons inside the nuclear fireball. The K^+ mesons are expected to be repelled from the bulk of nucleons due to the repulsive K^+N potential. The appropriate observable for this effect is the azimuthal emission pattern which reflects the collision geometry.

Figure 7 sketches the nuclear matter distribution in a semi-central Au+Au collision at 1 AGeV for the time steps 6.5 fm/c, 12.5 fm/c and 18.5 fm/c as calculated by a QMD transport code [32]. The trajectories of target and projectile define the reaction plane. This collision system was studied by the KaoS Collaboration which measured the azimuthal angular distributions of protons, pions and kaons. The particles were detected at a laboratory angle of $\Theta_{lab} = 84^\circ$ corresponding to a rapidity interval of $0 \leq y/y_{proj} \leq 0.2$. The direction to the spectrometer is indicated in figure 7 by the arrows.

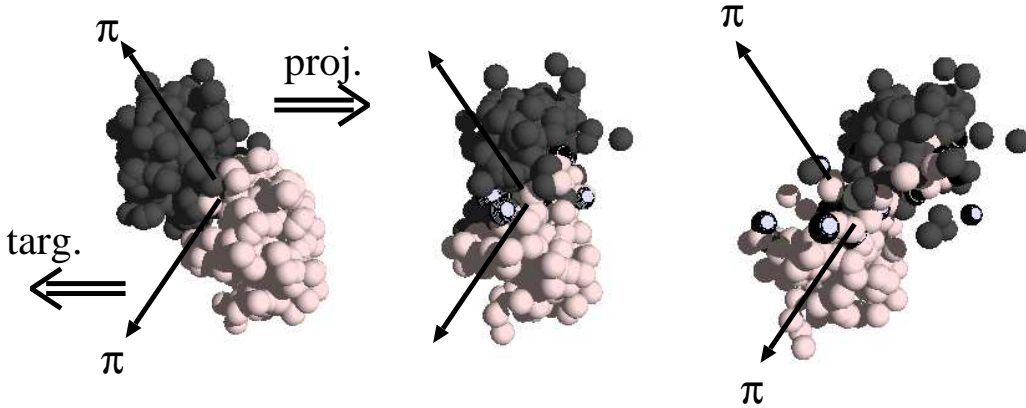


Figure 7. Sketch of an Au+Au collision at 1 AGeV with an impact parameter of 7 fm as calculated by a QMD transport code [32]. The snapshots are taken at 6.5 fm/c (left), 12.5 fm/c (middle) and 18.5 fm/c (right). The arrows indicate the position of the spectrometer at target rapidity.

The azimuthal emission pattern of protons, pions and K^+ mesons as measured in semi-central Au+Au collisions at 1 AGeV are shown in figure 8 [33]. The data are analyzed for impact parameters of $b > 5$ fm and transverse momenta of $0.25 \text{ GeV}/c < p_t < 0.75 \text{ GeV}/c$. The reaction plane is defined by the azimuthal angles $\phi = 0^\circ, 180^\circ$ together with the beam axis. A dip in the angular distribution around $\phi = 0^\circ$ corresponds to a predominant in-plane emission (so-called sideward flow) whereas the bumps at $\phi = \pm 90^\circ$ reflect an enhanced emission perpendicular to the reaction plane. The solid lines represent the Fourier expansion

$$dN/d\phi \propto [1 + 2v_1 \cos(\phi) + 2v_2 \cos(2\phi)]$$

which is fitted to the measured azimuthal distributions. The Fourier coefficients

$v_1 = \langle \cos(\phi) \rangle$ and $v_2 = \langle \cos(2\phi) \rangle$ characterize the strength of the emission side-wards (in-plane) and out-of-plane, respectively.

The proton distributions exhibit a very pronounced sideward flow signal. The pions are preferentially emitted perpendicular to the reaction plane. This effect is caused by the spectator fragments which shadow the pions emitted in-plane (see figure 7). The preferential in-plane emission of K^+ mesons indicates that the bulk of the K^+ mesons is emitted early, before the target spectator is able to shadow the kaons. From figure 7 one can estimate that the shadowing by the target spectator sets in after approximately 15 fm/c. This result is in remarkable agreement with the time evolution of kaon production as calculated by transport models (see figure 2). The kaon flow signal is even more pronounced than the flow signal of the high-energy pions which are not shown in figure 8 [34]. This effect indicates that K^+ mesons are strongly repelled from the participant and spectator matter.

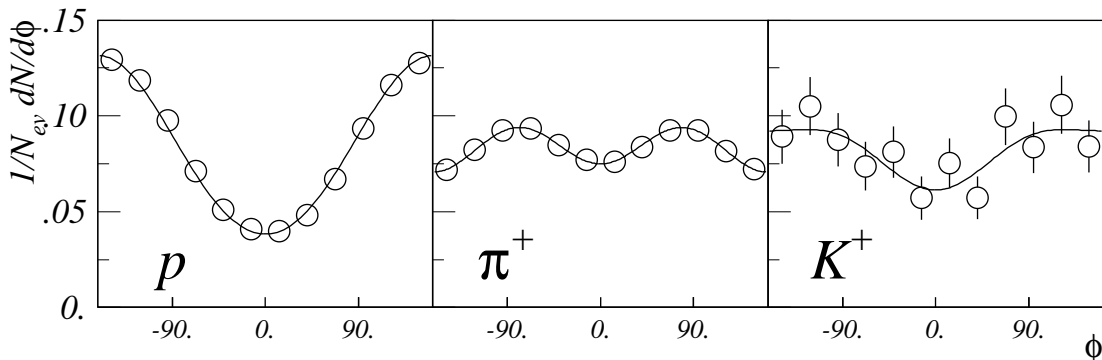


Figure 8. Azimuthal angle distribution of protons (left), pions (center) and K^+ mesons (right) measured in Au+Au collisions at 1 AGeV around target rapidity by the KaoS Collaboration [33]. The accepted range in transverse momentum is $0.25 \text{ GeV}/c < p_t < 0.75 \text{ GeV}/c$. The solid line represents a Fourier expansion fitted to the data (see text)

The FOPI Collaboration has studied the directed flow of kaons in more detail. Figure 9 shows the v_1 coefficient for protons (triangles) and K^+ mesons (dots) as function of transverse momentum measured in semi-central (left) and central (right) Ru+Ru collisions at 1.69 AGeV [21]. The data are taken around target rapidities. It can be seen that in semicentral collisions the sign of v_1 is opposite for protons and low-momentum K^+ mesons, i.e the kaons exhibit "antiflow" below transverse momenta of about $p_t=0.35 \text{ GeV}/c$. This observation is explained within transport calculations by a repulsive K^+N potential of $U = 20 \text{ MeV}$ at saturation density (solid lines). In central collisions, the low-momentum K^+ mesons are emitted more or less isotropically and thus a weaker K^+N potential is required by the calculations in order to describe the data. It should be noted that the calculations fail to describe the proton data. This discrepancy and the simplified assumption of a momentum-independent in-medium potential deserve further theoretical efforts.

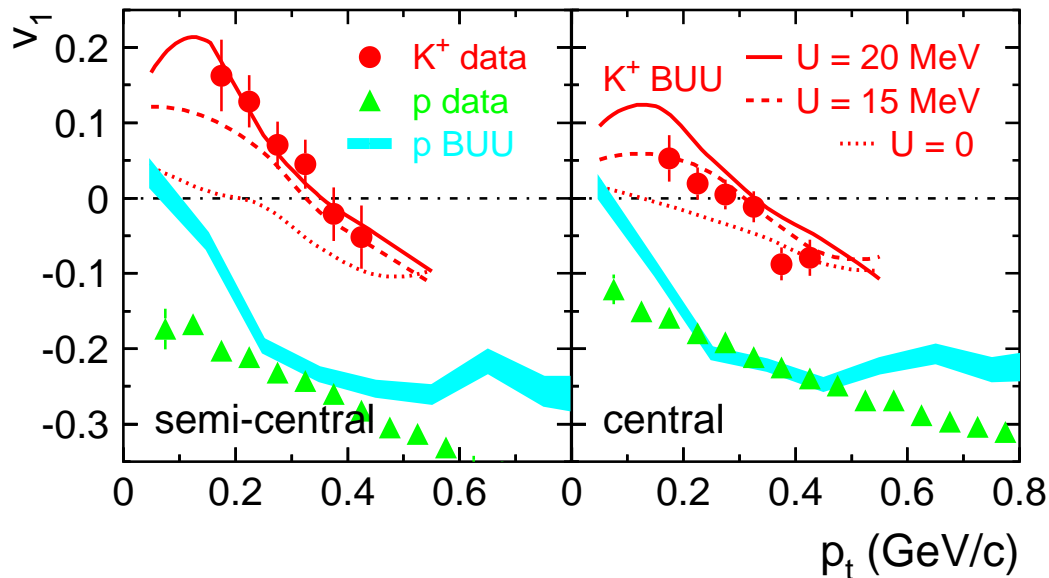


Figure 9. Flow coefficient v_1 for protons (triangles) and K^+ mesons (dots) versus transverse momentum p_t measured in semi-central (left) and central (right) Ru+Ru collisions at 1.69 AGeV by the FOPI Collaboration. The detector covers the rapidity range of $-1.2 < y^0 < -0.65$. The grey shadow illustrate protons from BUU calculations, the lines represent K^+ mesons calculated for different K^+N potentials as indicated. Taken from [21].

The KaoS Collaboration has measured the azimuthal emission pattern of K^+ mesons in Au+Au collisions at 1 AGeV around midrapidity [19]. Fig. 10 presents the $dN/d\phi$ distribution of kaons which were accepted within a range of transverse momenta of $0.2 \text{ GeV}/c \leq p_t \leq 0.8 \text{ GeV}/c$ for two ranges of normalized rapidities $0.4 \leq y/y_{proj} \leq 0.6$ (left) and $0.2 \leq y/y_{proj} \leq 0.8$ (right) with y_{proj} the projectile rapidity. The data are corrected for the uncertainty of the determination of the reaction plane on the basis of a Monte Carlo simulation.

The K^+ emission pattern clearly is peaked at $\phi = \pm 90^\circ$ which is perpendicular to the reaction plane. Such a behavior is known from pions [35] which interact with the spectator fragments. In the case of K^+ mesons, however, the anisotropy can be explained by transport calculations only if a repulsive in-medium K^+N potential is assumed. This is demonstrated by the solid lines in fig. 10. A flat distribution (dotted lines) is expected when neglecting the in-medium potential and only taking into account K^+ rescattering ([11], left) and additional Coulomb effects ([36], right).

In summary, the K^+ azimuthal emission pattern exhibits structures which contradict the naive picture of a long mean free path in dense nuclear matter. The particular features of sideward flow and the pronounced out-of-plane emission around midrapidity indicate that K^+ mesons are repelled from the nucleons as expected for a repulsive K^+N potential. The key observable for the study of KN potentials is the azimuthal emission pattern of

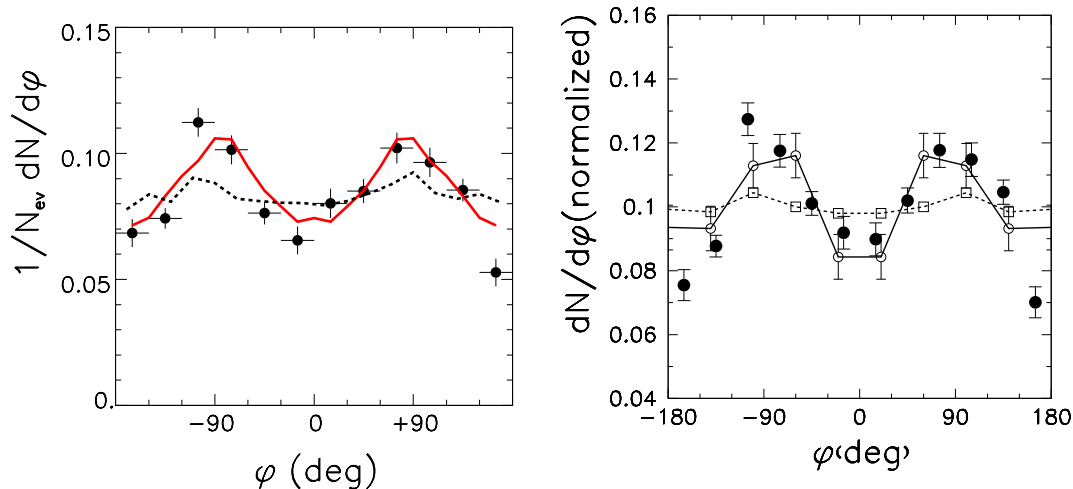


Figure 10. K^+ azimuthal distribution for semi-central Au+Au collisions at 1 AGeV (full dots). The data are analyzed at $0.4 < y/y_{proj} < 0.6$ (left) and $0.2 < y/y_{proj} < 0.8$ (right) [19]. The lines represent results of transport calculations from the Stony Brook group using a RBUU model (left [11]) and a QMD model from the Tübingen group (right [36]). Both models take into account rescattering, the QMD version also considers Coulomb effects. Solid lines: with in-medium KN potential. Dashed lines: without in-medium KN potential.

K^- mesons. If an attractive K^-N potential exists, the K^- mesons will be emitted almost isotropically in semi-central Au+Au collisions. This is in contrast to what one expects for a particle being absorbed in nuclear matter which is flowing nonisotropically [36]. Such an experiment has been performed by the KaoS Collaboration. The analysis is in progress.

5. K^+ production and the nuclear equation-of-state

Microscopic transport calculations claim that the yield of kaons created in collisions between heavy nuclei at subthreshold beam energies ($E_{beam} = 1.58$ GeV for $NN \rightarrow K^+\Lambda N$) is sensitive to the compressibility of nuclear matter at high baryon densities [37,38]. This sensitivity is due to the production mechanism of K^+ mesons. At subthreshold beam energies, the production of kaons requires multiple nucleon-nucleon collisions or secondary collisions such as $\pi N \rightarrow K^+\Lambda$ and $\Delta N \rightarrow K^+\Lambda N$. These processes are expected to occur predominantly at high baryon densities, and the densities reached in the fireball depend on the nuclear equation-of-state [39].

K^+ mesons are well suited to probe the properties of the dense nuclear medium because of the absence of absorption. They contain an antistrange quark and hence emerge as messengers from the dense phase of the collision. In contrast, the pions created in the high density phase of the collision are likely to be reabsorbed and most of them will leave the reaction zone in the late phase [40].

However, the K^+ yield does not only depend on the nuclear compressibility but also on the in-medium K^+N potential, as we have seen in the preceding sections. The KaoS

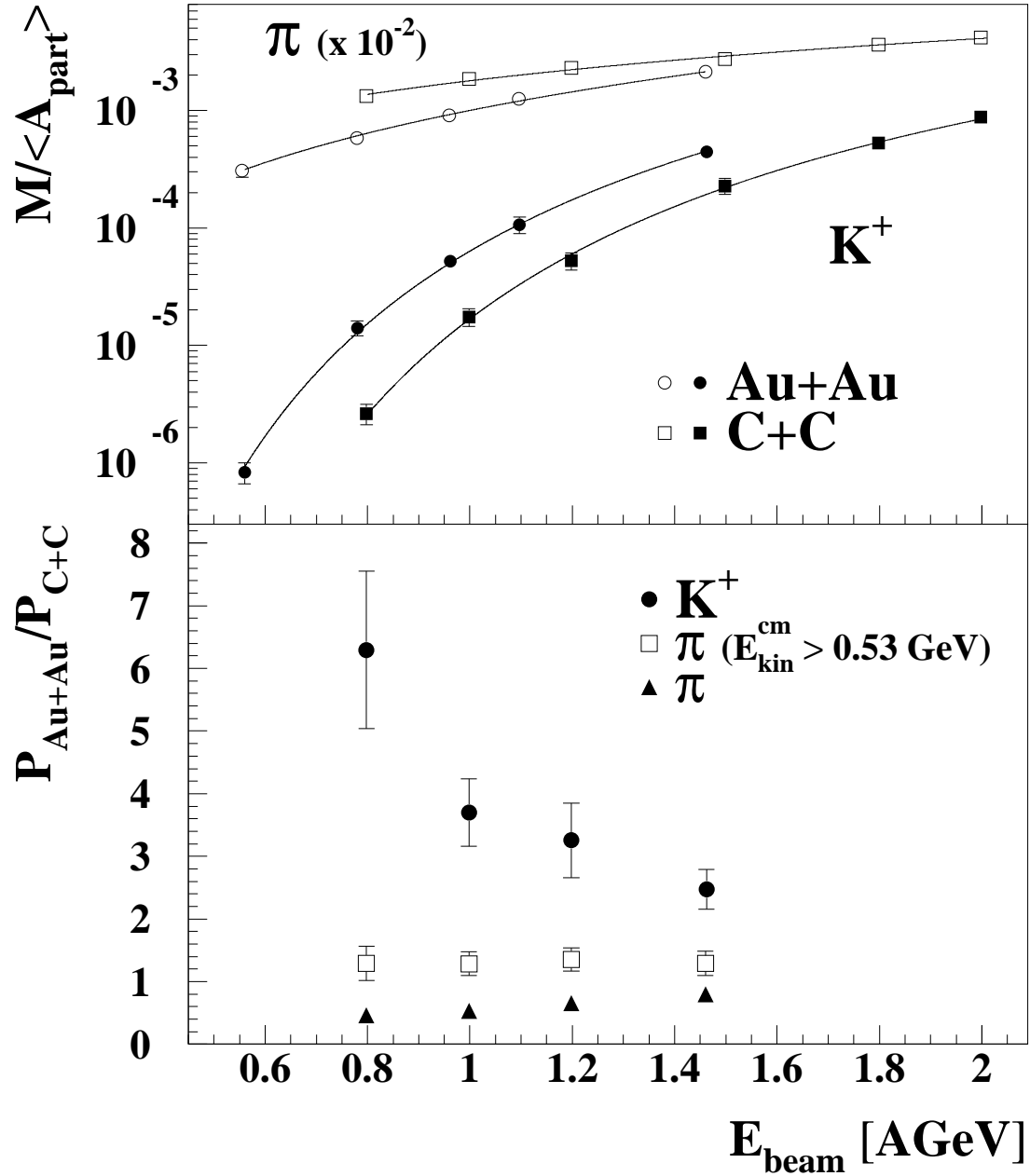


Figure 11. Upper panel: Pion and K^+ multiplicity per participating nucleon $P = M / \langle A_{part} \rangle$ for Au+Au and C+C collisions as function of the projectile energy per nucleon. The pion data include charged and neutral pions (see text). The lines represent a fit to the data. Lower panel: Ratio of the multiplicities per participant (Au+Au over C+C collisions) for K^+ mesons (full circles), pions (full triangles) and high-energy pions ($E_{kin}^{cm} > 530$ MeV, open squares) as function of the projectile energy per nucleon. Taken from [41].

Collaboration pursued the idea to disentangle these two effects by studying K^+ production in a very light ($^{12}\text{C}+^{12}\text{C}$) and a heavy collision system ($^{197}\text{Au}+^{197}\text{Au}$) at different beam energies near threshold [41]. In the heavy Au+Au system the average baryonic density - achieved by the pile-up of nucleons - is significantly higher than in C+C collisions [31]. Moreover, the maximum baryonic density reached in Au+Au collisions depends on the nuclear compressibility [2,38] whereas in the small C+C system this dependence is very weak [42]. Due to the fact that kaons are produced in multiple steps the kaon yield depends at least quadratically on the density. On the other hand, the repulsive K^+N potential is assumed to depend nearly (or less than) linearly on the baryonic density [3] and thus reduces the kaon yield accordingly. Therefore, the influence of the nuclear compressibility on the K^+ yield in Au+Au collisions should be measurable, and this effect is expected to increase with decreasing beam energy.

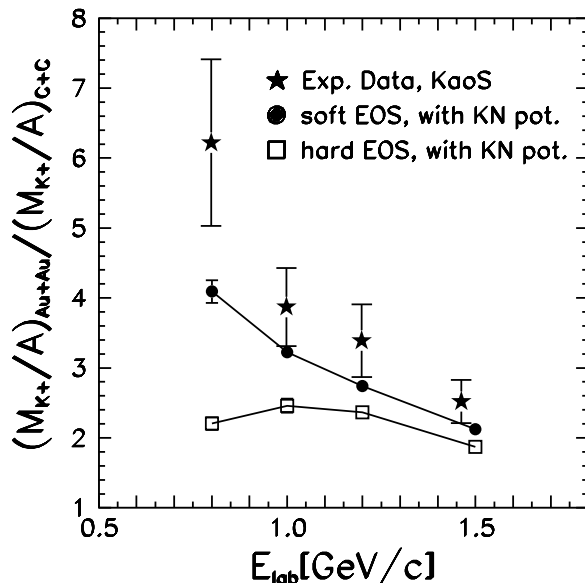


Figure 12. K^+ multiplicity ratio P_{Au+Au}/P_{C+C} as function of the beam energy for inclusive reactions. The data (stars) are compared to results of QMD transport model calculations based on a soft (full dots) and a hard (open squares) nuclear equation-of-state [42].

The multiplicity of K^+ mesons has been measured in inclusive C+C collisions at beam energies between 0.8 and 2 AGeV [20] and in inclusive Au+Au collisions between 0.6 and 1.5 AGeV [41]. The upper panel of figure 11 shows the inclusive pion and K^+ multiplicity per average number of participating nucleons $M / \langle A_{part} \rangle$ for C+C and Au+Au collisions as a function of beam energy. The average number of participating nucleons is given by $\langle A_{part} \rangle = A/2$ according to a geometrical model. The lower panel of figure 11 presents the ratios of the particle multiplicities measured in Au+Au and C+C collisions P_{Au+Au}/P_{C+C} with $P = M / \langle A_{part} \rangle$. The pion ratio (triangles) is well below unity which indicates pion absorption in the heavy system. In contrast, the K^+ mesons ratio P_{Au+Au}/P_{C+C} (full dots) is above two and still increases with decreasing beam energy.

Recently, the K^+ ratio P_{Au+Au}/P_{C+C} has been calculated also for inclusive reactions with QMD transport models [42,43]. Figure 12 shows the results of calculations [42] which are performed with two values for the compression modulus: $\kappa = 200$ MeV (a "soft")

equation-of-state, full dots) and $\kappa = 380$ MeV (a "hard" equation-of-state). These calculations take into account a repulsive kaon-nucleon potential and use momentum-dependent Skyrme forces. Figure 12 clearly demonstrates that the calculation based on a soft equation-of-state reproduces the trend of the experimental data (stars). The ratio P_{Au+Au}/P_{C+C} has the advantage that many uncertainties of both the model calculation and the experiment cancel in this presentation. Therefore, it is a promising task to improve the model inputs in order to achieve better agreement with the data.

6. Conclusions and outlook

We have presented data on the production and propagation of strange mesons in heavy-ion collisions in the SIS energy range. The K^-/K^+ ratio as function of the Q-value was found to be a factor of 10 - 100 larger in nucleus-nucleus than in proton-proton collisions. The K^-/K^+ ratio is almost independent of the size of the collision system although the absorption probability of K^- mesons should dramatically increase with increasing system size. These observations indicate that the yield of K^- mesons is enhanced and/or their absorption is reduced in dense nuclear matter. According to transport model calculations, the enhanced yield of K^- mesons is caused by their reduced effective mass in the medium. In Au+Au collisions at 1 AGeV, the K^+ mesons are emitted preferentially into the reaction plane at target rapidities and out-of-plane at midrapidity. In Ru+Ru collisions at 1.69 AGeV, the low momentum K^+ mesons are preferentially emitted opposite to the nucleons. These effects are explained within transport calculations by a repulsive K^+N potential.

The measurement of the K^- azimuthal emission pattern is considered to be a key experiment in this respect: if a strongly attractive K^-N potential exists, K^- mesons will be emitted almost isotropically although the nucleons are flowing nonisotropically in a semicentral nucleus-nucleus collision. More information on the in-medium properties of kaons and antikaons can be expected from production yields in proton-nucleus collisions. Both experiments have been performed by the KaoS Collaboration, and their analysis is in progress.

In the fall of this year the new Dilepton Spectrometer HADES at SIS/GSI will take first data. This will open a new era of studies of vector mesons and hadron properties in dense nuclear matter.

7. Acknowledgement

I would like to thank J. Aichelin, E. Bratkovskaya, W. Cassing, C. Fuchs and M. Lutz for valuable discussions. I thank the members of the FOPI Collaboration P. Crochet, A. Devismes, R. Kutsche and W. Reisdorf for supplying me with their data. It is a pleasure to thank my colleagues from the KaoS Collaboration who measured and analyzed most of the data presented in this article: I. Böttcher, A. Förster, E. Grosse, P. Koczon, B. Kohlmeyer, M. Menzel, L. Naumann, H. Oeschler, E. Schwab, W. Scheinast, Y. Shin, H. Ströbele, C. Sturm, F. Uhlig, A. Wagner and W. Waluś.

REFERENCES

1. G.E. Brown et al., Phys. Rev. **C 43** (1991) 1881

2. J. Aichelin, Phys. Rep. **202** (1991) 233
3. J. Schaffner-Bielich, J. Bondorf, I. Mishustin, Nucl. Phys. **A 625** (1997) 325
4. T. Waas, N. Kaiser and W. Weise, Phys. Lett. **B 379** (1996) 34
5. M. Lutz, Phys. Lett. **B 426** (1998) 12
6. G.E. Brown and H.A. Bethe, Astrophys. Jour. **423** (1994) 659 and Nucl. Phys. **A 567** (1994) 937
7. G.Q. Li, C.H. Lee and G.E. Brown, Phys. Rev. Lett. **79** (1997) 5214
8. H. Heiselberg and M. Hjorth-Jensen, Phys. Rep. **328** (2000) 237
9. E. Friedman and A. Gal, Phys. Lett. **B 308** (1993) 6
10. E. Friedman et al., Phys. Rev. **C 55** (1997) 1304
11. G.Q. Li, C.M. Ko and G.E. Brown, Phys. Lett. **B 381** (1996) 17
12. P. Senger et al., Nucl. Instr. Meth. **A 327** (1993) 393
13. A. Gobbi et al., Nucl. Instr. Meth. **A 324** (1993) 156
14. D. Miśkowiec et al., Phys. Rev. Lett. **72** (1994) 3650
15. J.Ritman et al., Z. Phys. **A 352** (1995) 355
16. W. Ahner et al., Phys. Lett. **B 393** (1997) 31
17. R. Barth et al., Phys. Rev. Lett. **78** (1997) 4007
18. D. Best et al., Nucl. Phys. **A 625** (1997) 307
19. Y. Shin et al., Phys. Rev. Lett. **81** (1998) 1576
20. F. Laue, C. Sturm et al., Phys. Rev. Lett. **82** (1999) 1640
21. P. Crochet et al., Phys. Lett. **B 486** (2000) 6
22. X.S. Fang, C.M. Ko, G.Q. Li, Y.M. Zheng, Nucl. Phys. **A 575** (1994) 766
23. M. Mang, PhD thesis, IKF, Univ. Frankfurt (1997)
24. M. Menzel et al., to appear in Phys. Lett. **B** (2000)
25. A. Sibirtsev, Phys. Lett. **B 359** (1995) 29
26. E.Bratkovskaya, W.Cassing and U.Mosel, Nucl.Phys. **A 622** (1997) 593
27. A. Sibirtsev, W. Cassing and C.M. Ko, Z. Phys. **A 358** (1997) 101
28. A. Förster, PhD Thesis in preparation, TU Darmstadt
29. K. Wisniewski et al., submitted for publication.
30. G.Q. Li and G.E. Brown, Phys. Rev. **C 58** (1998) 1698
31. W. Cassing and E. Bratkovskaya, Phys. Rep. **308** (1999) 65
32. C. Hartnack, private communication
33. I.M. Böttcher, PhD Thesis, Univ. Marburg (2000)
34. A. Wagner et al., Phys. Rev. Lett. **85** (2000) 18
35. D. Brill et al., Z. Phys. **A 357** (1997) 207
36. Z.S. Wang et al., Eur. Phys. J. **A 5** (1999) 275
37. J. Aichelin, C.M. Ko, Phys. Rev. Lett. **55** (1985) 2661
38. G.Q. Li, C.M. Ko, Phys. Rev. **C 54** (1996) R2159
39. C. Fuchs et al., Phys. Rev. **C 56** (1997) R606
40. S. Bass et al., Phys. Rev. **C 50** (1994) 2167
41. C. Sturm et al., submitted for publication
42. C. Fuchs et al., submitted for publication
43. C. Hartnack, J. Aichelin, Proc. of the VVVIII Int. Workshop in Hirschegg, Jan. 16-22, 2000 (1999) 65